

OMAE2014-24184

EXPERIMENTAL INVESTIGATION OF COMPRESSIVE FAILURE OF TRUNCATED CONICAL ICE SPECIMENS

Kashfi B. Habib

Memorial University of Newfoundland,
St. John's, NL, Canada

Rocky S. Taylor^{1,2}

¹Memorial University of Newfoundland,
²C-CORE Centre for Arctic Resource
Development
St. John's, NL, Canada

Ian J. Jordaan

Memorial University of Newfoundland,
St. John's, NL, Canada

Stephen Bruneau

Memorial University of Newfoundland,
St. John's, NL, Canada

ABSTRACT

A series of small-scale ice indentation tests has been carried out to study the compressive failure of polycrystalline ice during indentation and explore the link between various parameters that influence the ice failure processes. In total, twenty-eight experiments were completed using ice specimens having a truncated conical geometry to investigate the nature of crushing, spalling and high pressure zones. Variables considered in this series include: grain size, indenter shape, indentation rate, temperature, and taper angle. Two grain size ranges (0-4 mm and 4-10⁺ mm) were considered, along with two indenter shapes (a flat plate and a spherical indenter). Indentation rates of 0.1 mm/s, 1 mm/s and 10 mm/s have been used for these tests. Experiments were conducted at temperatures of -10°C and -5°C and three geometric configurations (with taper angles of 13°, 21°, 30°) have been considered. Crushing and spalling events have been observed from the regular and high-speed videos, synchronized with tactile pressure sensor data and load cell data. To observe the microstructural modification, horizontal and vertical thin-sections of the damaged ice adjacent to the indenter have been collected and examined. Ice particles were collected from the testing area following each experiment to observe the influence of different factors. Particle size distributions and post-experiment image analyses were also conducted after each test. The effect of the variables on observed failure processes and associated loads are discussed.

INTRODUCTION

Sea ice and icebergs present significant challenges for the development of arctic and subarctic oil and gas resources in northern regions. Offshore structures and vessels must be designed to withstand interaction with such ice features, which may fail in different types of modes such as compressive ice failure, flexural failure, spalling, buckling, crushing or any combination of these failure modes. For vertical-walled structures, compressive failure during the interaction with ice features can result in high local loads and dynamic response in the structures potentially leading to load amplification and fatigue issues. Other concerns such as resonance, durability and serviceability must also be considered in the design process.

Compressive ice failure is associated with two primary load limiting mechanisms: spalling fracture and microstructural damage. Spalling is particularly important in the localization of contact during an interaction and plays a dominant role in shaping the edge of the ice feature at the ice-structure interface. Crushing processes are associated with 'damage' mechanisms such as microfracture, recrystallization and localized pressure melting, which result in significant changes to ice material behavior and also play an important role in the formation and development of a layer of highly damage ice adjacent to the structure (Jordaan, 2001). These mechanisms are responsible for the formation of one of the most important elements of the

interaction process during compressive ice loading: the high pressure zone (*hpz*). These *hpzs* are localized zones of intense pressure resulting from the localization of contact and through which the majority of load is transmitted to the structure (Jordaan, 2001). From tactile sensor data it has been observed that for interactions with level ice, *hpzs* only cover approximately 10% of the global interaction area (Frederking, 2004; Taylor et al., 2008).

Damage-related crushing results in the pulverization and extrusion of softened ice from the periphery of contact zones, which can produce repeated load fluctuations, leading to the failure of individual high pressure zones. The extrusion of crushed ice from the contact interface is highly dependent on localized damage processes within the *hpzs*, which are a function of temperature, strain rate and the triaxial state of stress (Meglis et al., 1999, Melanson et al., 1999, Xiao, 1997; Barrette et al., 2002; Wells et al., 2010). Spalling fracture is associated with a significant asymmetric loss of contact area at the ice-structure interface due to removal of a discrete piece of ice, which in turn causes a sudden load drop. Spalling tends to be more dependent on the elastic stress field behind the damaged layer and the distribution of flaws within the ice (Taylor et al., 2008). Since this stress field within the ice is dependent on the geometry of the ice feature, which evolves throughout an interaction, understanding the influence of specimen shape on damage and fracture mechanisms is also an important consideration to aid in the development of representative models of ice loads during ice-structure interactions.

Prior experimental evidence indicates that similitude exists for damage layers over a wide range of geometric scales (Barrette et al., 2002; Jordaan et al., 2012). Provided that the displacement rate is scaled according to the scaling constant λ , the solution for the development of the layer should be identical at different scales. In the present work, this insight is the basis for use of small-scale experiments to study scaled high pressure zones for conical ice specimens. Prior experimental work on ice indentation provide important background to the research presented herein (see for example, Barrette et al. 2002; Wells et al., 2010; Browne et al., 2013; Browne, 2012, Taylor et al., 2013; Dillenburg, 2012; Bruneau et al., 2011, 2012, 2013; Sullivan and Pilling, 2011; Dragt and Bruneau, 2013). In the present program, laboratory experiments have been used as a cost-effective means to study the influence of indentation rate, temperature and grain size on fracture and damage processes during the indentation of conical ice specimens using flat and curved indenters. In the sections below, a summary of results from recent laboratory experiments have been provided; the reader is referred to Habib (2014) for additional details.

EXPERIMENTAL SETUP

To produce the ice specimens, commercially purchased freshwater, polycrystalline ice was crushed into ice seed using an industrial ice crusher and sieved into two different size ranges: 0-4 mm and 4-10⁺ mm. The specimens produced were taken to be representative of glacial or multi-year ice that has equiaxed, randomly oriented grains, which can be considered statistically isotropic. Water for these ice samples was prepared by distillation, deionization and deaeration processes. The compacted water and ice mixture were set into a mold and placed into the freezer at -25°C. The bottom portion of the mold also served as a confining ring, which remained affixed to the ice during the crushing tests. After two days of freezing, the samples were shaped using an ice shaping apparatus. As illustrated in Figure 1, conical truncated ice specimens were used with an average diameter of 268.8 mm at the bottom and 25.4 mm at the top. Three ice specimen taper angles were considered: 13°, 21° and 30°. After shaping, the ice specimens were covered and stored in the cold room for at least twenty-four (24) hours to adjust it to the desired temperature (Jones et al., 2003). Details of the water and ice preparation processes used may be found in Bruneau et al. (2011).

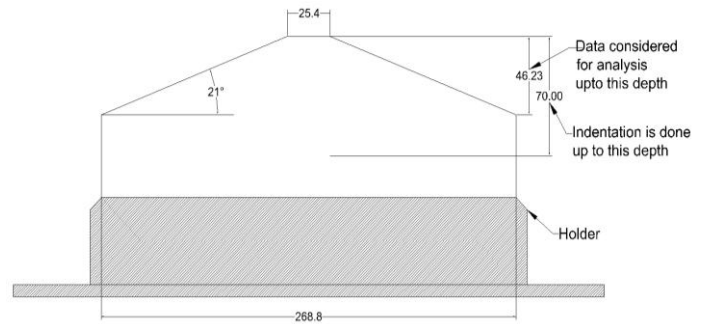


Figure 1: Geometry of ice specimen having taper angle 21° (all dimensions are in mm)

For this test program, the Materials Testing System (MTS) at Memorial University of Newfoundland was used. For a given experiment, the indenter plate was mounted to the primary load cell, which was fixed to the MTS cross-head. During testing, the shaped ice specimens were mounted on the MTS base plate, which was attached to the hydraulic ram. The hydraulic ram was used to control vertical displacement and the indentation rate of the mounted ice specimen, while the indenter plate and MTS crosshead remained fixed. Before each test was conducted the ice specimen was brought as close as possible to the indenter.

To provide additional insight into the nature and variation of contact pressures, Tekscan tactile pressure sensors were placed at the ice-indenter interface. The handles for these sensors were

mounted on the MTS machine with clamps, so as to keep the sensor straight and fixed along the indenter plate as the ice specimen moved upward as shown in Figure 2.

The indentation for each test was done from the top surface of the ice sample to a depth of 70 mm. During the analysis, only data up to the conical edge of the ice sample were considered. The data collected from the MTS load cell were the force against indentation depth and time.

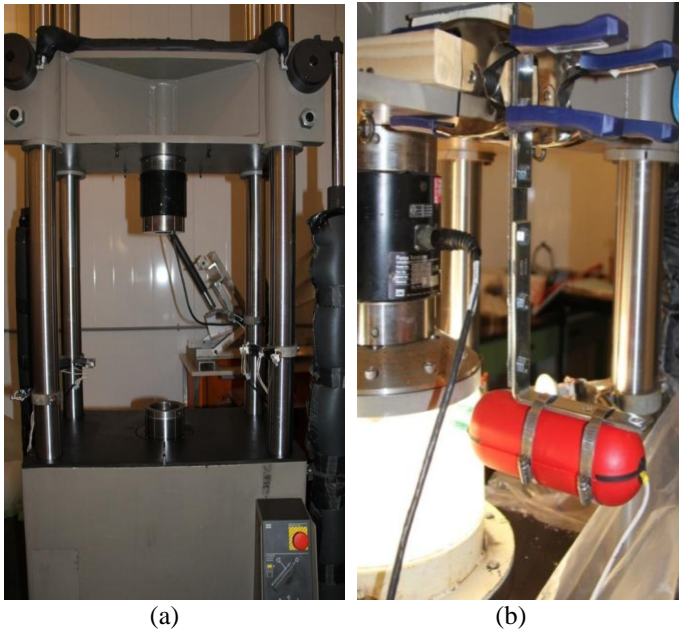


Figure 2: (a) MTS load frame (b) Arrangement of Tekscan sensor with MTS load frame

Regular and high-speed video recordings were also collected to capture the crushing behavior and failure mechanisms during the indentation tests. To assess the distribution of particle sizes associated with these tests, spalled ice pieces were collected, sieved and weighed. Thin-sections of the damaged and parent ice were also prepared using the Sinha (1977) double-microtome technique to study the internal structures and grain size distributions of ice. These thin sections also helped provide insight into the characteristics of the damaged layer and associated processes.

RESULTS AND DISCUSSION

In total twenty-eight (28) experiments were completed. These experiments were done at two different temperatures. Twenty-four (24) tests were done at -10°C and four (4) tests were done at -5°C . As described by Jones et al. (2003), iceberg temperatures vary from 0°C to -10°C from the surface of the ice

to a depth of 1-2 meters, and understanding the influence of such variations in temperature on ice failure processes is essential. The test matrix of the experiments is given in Table 1.

Table 1: Test Matrix

Test No	Test ID	v	α	G	T	Indenter
1	T01_0.1_21_1_10_F	0.1	21	4-10 ⁺	-10	Flat
2	T02_0.1_21_2_10_F	0.1	21	0-4	-10	Flat
3	T03_1_21_1_10_F	1	21	4-10 ⁺	-10	Flat
4	T04_10_21_1_10_F	10	21	4-10 ⁺	-10	Flat
5	T05_1_21_2_10_F	1	21	0-4	-10	Flat
6	T06_10_21_2_10_F	10	21	0-4	-10	Flat
7	T07_10_21_2_10_S	10	21	0-4	-10	Spherical
8	T08_10_21_1_10_S	10	21	4-10 ⁺	-10	Spherical
9	T09_10_30_1_10_S	10	30	4-10 ⁺	-10	Spherical
10	T10_10_30_2_10_S	10	30	0-4	-10	Spherical
11	T11_0.1_30_1_10_F	0.1	30	4-10 ⁺	-10	Flat
12	T12_10_30_2_10_F	10	30	0-4	-10	Flat
13	T13_1_30_1_10_F	1	30	4-10 ⁺	-10	Flat
14	T14_1_30_2_10_F	1	30	0-4	-10	Flat
15	T15_10_30_1_10_F	10	30	4-10 ⁺	-10	Flat
16	T16_0.1_30_2_10_F	0.1	30	0-4	-10	Flat
17	T17_0.1_13_1_10_F	0.1	13	4-10 ⁺	-10	Flat
18	T18_0.1_13_2_10_F	0.1	13	0-4	-10	Flat
19	T19_1_13_1_10_F	1	13	4-10 ⁺	-10	Flat
20	T20_1_13_2_10_F	1	13	0-4	-10	Flat
21	T21_10_13_1_10_F	10	13	4-10 ⁺	-10	Flat
22	T22_10_13_2_10_F	10	13	0-4	-10	Flat
23	T23_10_13_1_10_S	10	13	4-10 ⁺	-10	Spherical
24	T24_1_13_1_10_S	1	13	4-10 ⁺	-10	Spherical
25	T25_0.1_21_1_5_F	0.1	21	4-10 ⁺	-5	Flat
26	T26_1_21_1_5_F	1	21	4-10 ⁺	-5	Flat
27	T27_10_21_1_5_F	10	21	4-10 ⁺	-5	Flat
28	T28_10_21_2_5_F	10	21	0-4	-5	Flat

In the table, v is the indentation rate (mm/s); α is the taper angle (degrees); G is the grain size (mm); T is the temperature ($^{\circ}\text{C}$).

Effect of Indentation Rate

To investigate the effect of indentation rate, tests were done at speed of 0.1 mm/s, 1 mm/s and 10 mm/s. In Figure 3 force-displacement plots are given for three tests having different indentation rates up to the indentation depth of 10 mm. For the curve of the slow test (0.1 mm/s) it was observed that that the sample has experienced slow crushing failure with a continuously increasing load, which corresponds with the production of a slow, continuous flow of highly damaged crushed from beneath the contact zone and which is often referred to as a 'ductile' failure mode. In the medium speed test (1 mm/s) the ice has experienced a brittle failure with a large amount of cyclic loading during the first few seconds, and then it began to experience a 'ductile' failure with steadily increasing load. In the fast speed test (10 mm/s) the load initially builds for the first few millimetres of indentation depth, after which regular patterns of cyclic loadings are observed.

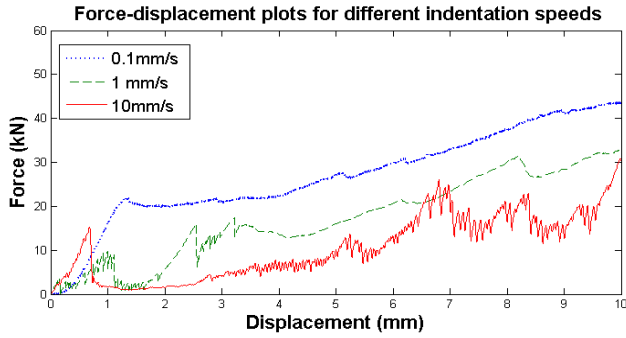


Figure 3: MTS load cell data for the three tests at different speeds: Slow speed test (Test 2: blue); Medium speed test (Test 5: green); Fast speed test (Test 6: red)

Vertical thin-section pictures in Figure 4 illustrate the extent of microstructural modification at three different indentation rates. Each section is 40 mm in height and 20 mm in width. The thin-sections for the slow test show that the sample is heavily dominated by recrystallization and microfracture, with the depth of the damaged area about 35 mm in length. Recrystallized ice is observed as having a much smaller grain size as compared to the parent ice, while microstructure appear as white lines when subjected to side lighting as shown in figure. In the case of the medium speed test both recrystallization and microfracture have an effect to a depth of about 15-20 mm and in case of the fast speed test recrystallization and microfracture are concentrated in the immediate crushing zone, and only extend to a depth of few millimeters.

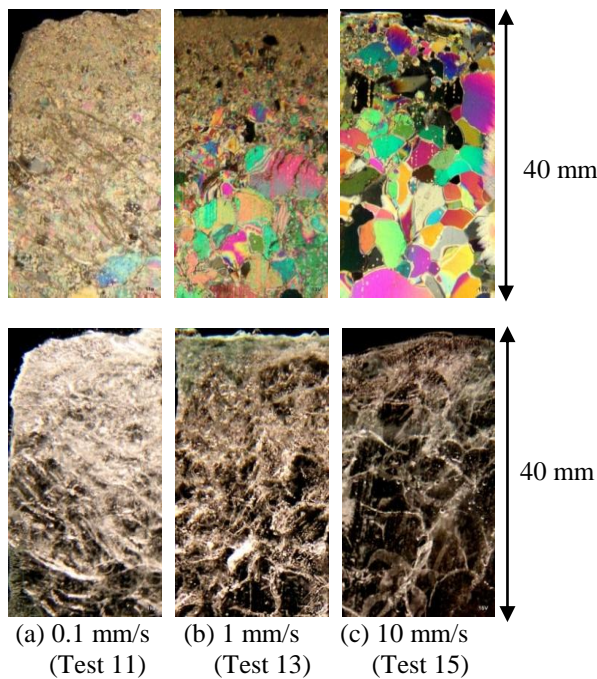
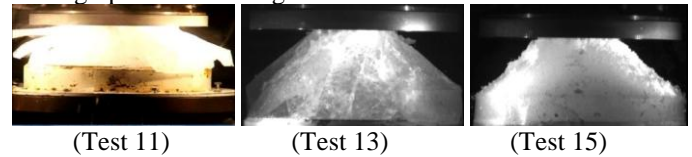


Figure 4: Vertical thin-section pictures showing the effect of indentation rate using cross polarized light (top) and side light (bottom)

Figure 5 shows photographs of the specimens during the indentation and immediately after crushing for the tests previously discussed. In case of the slow speed test, the image during indentation shows clear evidence of slow crushing and damage enhanced creep and the after crushing image shows a very smooth finish with no spall on the top of the ice sample. The medium speed test images taken during and after the test show both damage and fracture failure. In the center of the crushed sample, there is clear evidence of extreme and highly damaged failure of ice which has a smooth surface, but the spalled areas near the edges have much rougher and more irregular surfaces. The image taken during the fast test shows crushing and spalling occurring simultaneously. The image taken after crushing shows that the ice has characteristics of brittle failure with a rough and irregular surface at the final stage of the test and a smaller zone of localized damage. Such fast tests typically produced many small spalls and fractured ice pieces.

Photographs taken during the tests:



Photographs taken after the tests:



Figure 5: Photographs of during (top) and after crushing (bottom) for tests at three different indentation speeds

The total spall masses as a function of taper angle are presented in Figure 6 for different indentation rates. From this plot it is observed that the total spall mass is observed to be less for the slow tests than for the faster tests, since the ice has enough time to dissipate energy through damage-enhanced creep and these mechanisms dissipate adequate energy to prevent local fractures. By comparison, the medium and fast tests were observed to result in the production of a larger total spall masses. The results also show that the 13° taper angle ice samples have more spalls than those of 21° and 30° ice samples have fewer spalls than those of 21° ice sample. Part of the reason for these results may be attributed to the fact that the 13° taper angle ice samples had more initial mass than the other two, while the 30° ice samples had less initial mass due to its shape. Initially the average mass of the undeformed specimens were 11.4 kg for 13°, 9.8 kg for 21° and 9.1 kg for 30° taper angle ice samples. These differences in initial mass account for part of the differences observed in Figure 6, however not fully.

Based on this observation it is concluded that the geometry did have an effect on the amount of spalling that occurred.

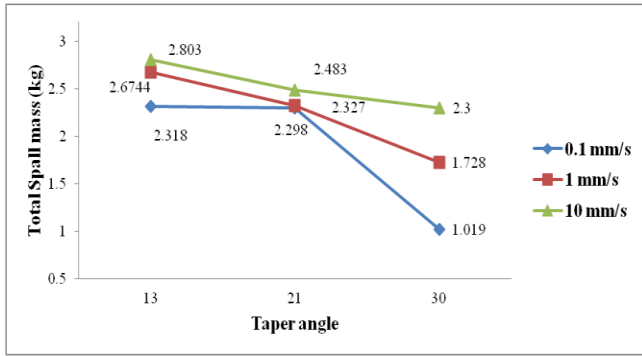


Figure 6: Total spall masses for ice crushing tests at different indentation speeds and taper angle

Effect of Temperature

The effect of temperature can be observed from the force-displacement plots of fast indentation tests at two different temperatures given in Figure 7. From this result it is observed that the warm test (-5°C) exhibits more ductile failure, dominated by damage, while the cold test (-10°C) experiences more brittle failure. It should be noted that the large load drops still occur in the warm tests due to spalling events, but there are fewer cyclic loadings in this case.

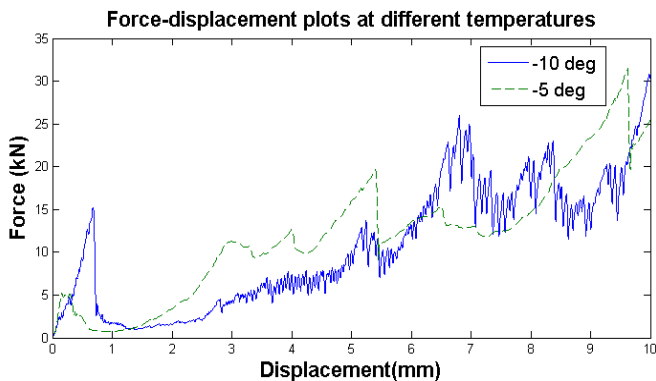


Figure 7: Load cell data for tests at different temperatures: cold test at -10°C (Test 6) and warm test at -5°C (Test 28)

Vertical thin-section pictures in Figure 8 show clear evidence of the effect of temperature. Thin-section pictures taken using cross polarized light show that in warmer ice (-5°C) the damaged layer is more heavily dominated by recrystallization as compared to colder (-10°C) ice. From the pictures taken using side-lighting, it is observed that cold tests are dominated by zones of microfracture. The warm test also has some microfracture, but the depth of the damaged layer

appears to be larger in the case of the warm ice test than in the cold ice test. Barrette et al. (2002), Li et al. (2004) and Browne (2012) found similar observations in their research.

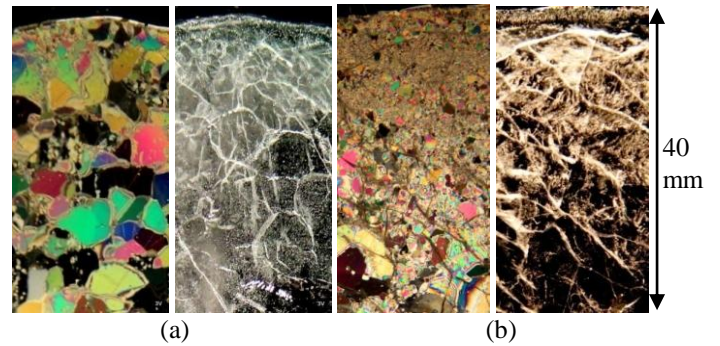


Figure 8: Vertical thin-section pictures using cross polarized light and side light (a) Cold test results at -10°C (Test 3) (b) Warm test results at -5°C (Test 26)

Images taken of the specimens after crushing are given in Figure 9 for the cold and warm ice specimens. The ice sample from the cold test shown in this figure is observed to have a rough and 'dry' looking surface with some small spalls on the top of the sample. By comparison, the ice sample from the warm test is observed to have a smoother, 'wet' surface appearance.



Figure 9: Photographs of after crushing samples at two different temperatures (a) -10°C (Test 6) (b) -5°C (Test 28)

Effect of Grain Size

For the test cases considered in these experiments, it was observed that grain size has a strong effect on the failure behavior. The force-displacement plots given in Figure 10 are for the ice samples with two grain size distributions conducted at -10°C. The samples had an indentation rate of 10 mm/s with a taper angle of 30°. For the ice sample made of smaller ice seeds (0-4 mm) less spalling fractures are observed, resulting in higher loads as compared to the specimen made of bigger ice seeds (4-10+ mm). From the plots, it can be seen that both tests exhibit cyclic loading for the first 3 millimeters of indentation depth, but after that, the sample with the bigger grain size

experiences a large failure with higher force. Then the sample continues to follow cyclic loadings with large load drops. However, the ice sample with smaller grain size continues to exhibit a continuous crushing with occasional large spalling events.

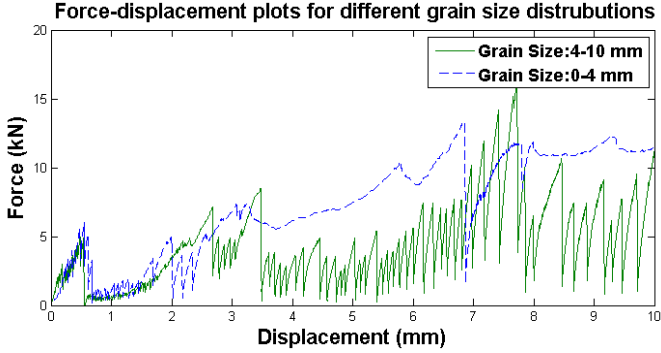


Figure 10: Load Cell data for two tests with different grain size
 Grain size distribution of 0-4 mm (Test 12)
 Grain size distribution of 4-10⁺ mm (Test 15)

Tactile pressure sensor data given in Figure 11 and corresponding force-time data given in Figure 12 show results for tests with two different grain sizes done at -5°C that were conducted at 10 mm/s on samples having taper angle of 21°. In Figure 11, the tactile pressure sensor images from event (a) to (e) show significantly higher pressures in case of smaller grain size ice sample than the bigger grain size ice sample with continuous change of contact area. Correspondingly, from the load cell data in Figure 12, the force in smaller grain size ice samples is generally observed to be higher, except at event (c) due to a spalling event at 0.57 s in the smaller grain size ice, which results in a drop in force and loss of contact area.

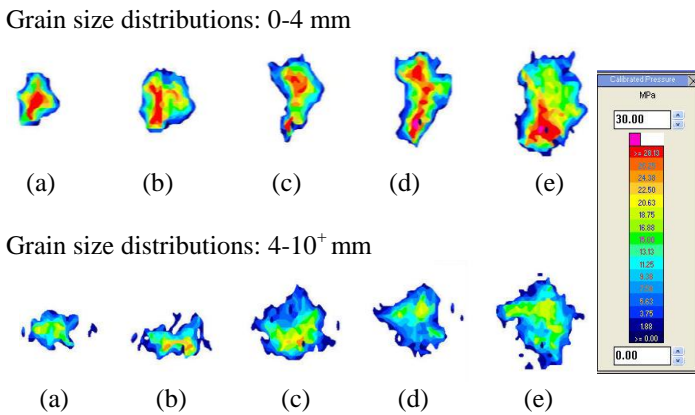


Figure 11: Pressure distribution images for tests having different grain size distributions.
 Top: Grain size distribution of 0-4 mm (Test 28);
 Bottom: Grain size distribution of 4-10⁺ mm (Test 27)

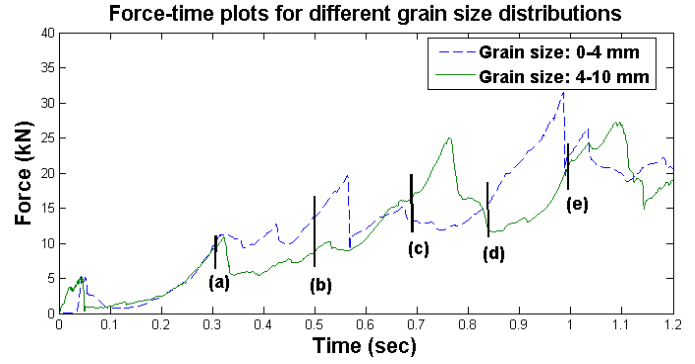


Figure 12: MTS load cell data corresponding to the pressure distribution images. Grain size distribution of 0-4 mm (Test 28) and 4-10⁺ mm (Test 27)

In Figures 13 and Figure 14 the thin-section pictures for horizontal and vertical sections are presented using cross polarized light and side-lighting techniques. From the horizontal thin-section pictures, the grain distributions corresponding to both grain-size ranges may be seen. Different color grains indicate that the crystallographic orientations of ice grains are different from each other and randomly distributed. The vertical thin-section pictures shown in Figure 14 correspond to medium speed tests done at -10°C and show that extensive microstructural damage may be observed in both, with a very high degree of microcracking in the smaller grain size specimen shown in Figure 14 (a).



Figure 13: Horizontal thin-section pictures defining the grain distribution using cross polarized light for grain size distributions (a) 0-4 mm (b) 4-10⁺ mm

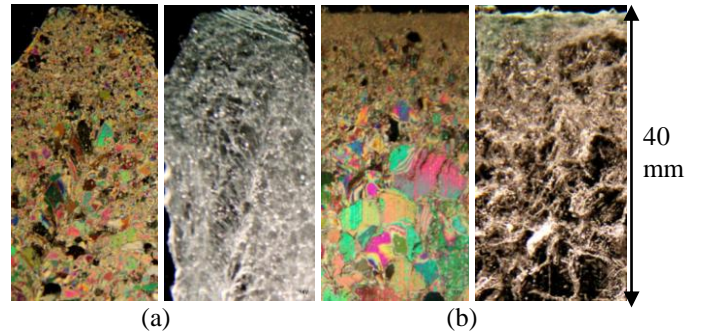


Figure 14: Vertical thin-section pictures using cross polarized light (color) and side light (black and white) for grain size distributions (a) 0-4 mm (Test 14); (b) 4-10⁺ mm (Test 13)

CONCLUSIONS

Small-scale laboratory tests have been conducted to improve the understanding of ice compressive failure during indentation of conical ice specimens. The main objective of this research was to investigate the nature of high pressure zones and the dependence of associated load limiting mechanisms (damage and fracture) on indentation rate, temperature and grain size.

From these experiments it was observed that during slow speed tests (0.1 mm/s), continuous crushing and damage enhanced creep (ductile) failure occurred throughout the indentation. During fast (10 mm/s) tests, brittle failure was frequently observed and often resulted in cyclic loading patterns. The medium (1 mm/s) speed tests have shown a combination of ductile and brittle behavior. As the indentation rates increase the amount of recrystallizations and microfractures decrease, showing significantly more recrystallizations and microfractures in the slow speed tests than in the medium and fast speed tests. In the slow speed tests fewer spalls were recorded than the other cases because damage-enhanced creep processes allow enough time to dissipate energy and prevent local fracture. During slow tests, when spalls did occur they tended to be quite large due to the time-dependent growth of large fractures.

Warm tests (-5°C) have shown an inclination towards ductile failure, and no significant cyclic loading patterns were observed during the warm tests. This lack of cyclic loading for warm ice was observed even for test cases that used the same test conditions which produced continuous cyclic loading pattern with large load drops in cold ice (-10°C). Thin-section pictures of warm tests have shown extensive damaged layers near the indentation edge that are heavily dominated by recrystallization. In the cold tests, the layers are observed to be dominated more by microfracture.

Ice specimens made of fine or smaller grain ice seeds (0-4 mm) appear to be stronger than samples made of coarse or bigger grain ice seeds (4-10⁺ mm). The average force and pressure are higher in the case of ice samples made of smaller ice seeds. From the thin-section pictures, ice samples with smaller ice seeds tend to have more extensive microstructural damage than their large grained counterparts.

Overall it is concluded that these experiments provide good agreement with fracture and damage mechanics theories, as well as with prior compressive ice failure studies. Further work to assess details of the spall size distributions, links between these distributions and the associated failure mechanisms is recommended. Further experimentation to assess repeatability of observed trends is also proposed.

ACKNOWLEDGMENTS

The authors would like to thank the following people: Mr. Craig Mitchell, Mr. Andrew Manuel, Mr. Sander Dragt and Mr. Brian O'Rourke for their assistance during laboratory testing at Memorial University of Newfoundland. The authors would also like to thank Memorial University for use of their cold room facilities and the STePS² for use of their apparatus. Financial support from the Research and Development Corporation of Newfoundland and Labrador (RDC) and the C-CORE Centre for Arctic Resource Development (CARD) are gratefully acknowledged.

REFERENCES

- Barrette, P., Pond, J., and Jordaan, I. (2002). Ice damage and layer formation in small scale indentation experiments. *Ice in the Environment, Proceedings of the 16th international Symposium on Ice, IAHR, Dunedin, New Zealand*, Volume. 3, Pages 246-253.
- Browne, T. (2012). Analysis of Compressive Ice Failure during Ice-structure Interaction. M. Eng Thesis. Memorial University of Newfoundland. St. John's, Canada .
- Browne, T., Taylor, R.S., Jordaan, I., Gürtner, A.,(2013). Small-scale Ice Indentation Tests with Variable Structural Compliance. *Cold Regions Science and Technology*, Volume 88, April 2013, Pages 2-9.
- Bruneau, S., Dillenburg, A., Ritter, S. (April, 2011). Ice Specimen Fabrication Techniques and Indentation Experiments, A STePS² Pilot Laboratory Investigation of Ice-Structure Interaction. STePS²-RP001-2011. Memorial University of Newfoundland, Sustainable Technology for Polar Ships and Structures, St. John's, NL, Canada , P. 139.
- Bruneau, S., Dillenburg, A., Ritter, S. (June, 2012). Ice Sample Production Techniques and Indentation Tests for Laboratory Experiments Simulating Ship Collisions with Ice. Rhodos, Greece.
- Bruneau, S., Colbourne, B., Dragt, R., Dillenburg, A., Ritter, S., Pilling, M., Sullivan, A. (June, 2013). Laboratory Indentation Tests Simulating Ice-Structure Interactions Using Cone-Shaped Ice Samples and Steel Plates. POAC. Espoo, Finland.
- Dillenburg, A. K. (2012). Rate dependency in conical ice indenter failure. Master's Thesis, University of Duisburg-Essen, Germany.
- Dragt, R.C., Bruneau, S.E. (2013). The Collision of Cone Shape Ice Samples against Steel Plates of Varying Surface Roughness. POAC. Espoo, Finland.
- Frederking, R. M. W. (2004). Ice pressure variations during indentation. *Proceedings of the 17th IAHR International Symposium on Ice*, Vol. 2. pp. 307.

Habib, K. B. (2014). Experimental Investigation of compressive failure of truncated conical ice specimen. Master's Thesis, Memorial University of Newfoundland, St. John's, Newfoundland, Canada.

Jones, S. J., Gagnon, R.E., Derradji, A., and Bugden, A. (2003). Compressive strength of iceberg ice. *Canadian Journal of Physics*.

Jordaan, I. J., Taylor, R. S., and Derradji-Aouat, A., (2012). Scaling of Flexural and Compressive Ice Failure. Proceedings of Offshore Mechanics and Arctic Engineering Conference (OMAE), Rio de Janeiro, Brazil.

Jordaan, I.J. (2001). Mechanics of ice-structure interaction. *Engineering Fracture Mechanics*; 68 , pp.1923-1960.

Li, C., Barrette, P., Jordaan, I.J. (2004). High Pressure Zones at Different Scales During Ice-Structure Indentation. Proceedings of 23rd International Conference on Offshore Mechanics and Arctic Engineering.

Meglis, I., Melanson, P., and Jordaan, I. (1999). Microstructural change in ice: II. creep behavior under triaxial stress conditions. *Journal of Glaciology* 45 (151) , 438–448.

Melanson, P.M., Meglis, I.L., Jordaan, I.J. and Stone, B.M. (1999). Microstructural change in ice: I. Constant-deformation-rate tests under triaxial stress conditions. *Journal of Glaciology*, Vol. 45, No.151, pp. 417-422.

Sinha, N.K., (1977). Technique for studying the structure of sea ice. *Journal of Glaciology*, Vol-18, pp. 315-323.

Sullivan, A. Pilling, M. (August, 2011). Influence of Ice Shapes on Indentation Loads. Work Term Report for STePS² program, Memorial University Division Of Cooperative Engineering.

Taylor, R.S., Browne, T., Jordaan, I., Gürtner, A., (2013). Fracture and Damage during Dynamic Interactions between Ice and Compliant Structures at Laboratory Scale. Proceedings of Offshore Mechanics and Arctic Engineering Conference, Nantes, France.

Taylor, R.S., Frederking, R, and Jordaan, I. J. (2008). The nature of high pressure zones in compressive ice failure. Proceedings 19th IAHR Symposium on Ice, Vancouver, British Columbia, Canada.

Wells, J., Jordaan, I., Derradji-Aouat, A. and Taylor, R. (2010). Small-scale laboratory experiments on the indentation failure of polycrystalline ice in compression: Main results and pressure distribution. *Cold Regions Science and Technology*, Vol. 65, No. 3 , pp. 314-325.

Xiao, J. (1997). Damage and fracture of brittle viscoelastic solids with application to ice load models. Ph. D Thesis, Memorial University, St. John's, NL, Canada.